

OPEN ACCESS

EDITED BY Carmine Izzo, University of Salerno, Italy

REVIEWED BY
Mary L. Taub,
University at Buffalo, United States
Alessio Mazzieri,
University of Perugia, Italy

*CORRESPONDENCE
Cheng Wang
wangch2@mail.sysu.edu.cn
Yongjie Jin
kimyg1118@sina.com

[†]These authors have contributed equally to this work

RECEIVED 29 April 2025
ACCEPTED 25 August 2025
PUBLISHED 15 September 2025

CITATION

Shi X, Zou W, Li X, Liu S, Hu T, Li Q, Zhang T, Chen L, Wu S, Wang C and Jin Y (2025) SGLT2 inhibition attenuates diabetic tubulopathy by suppressing SGK1-mediated pyroptosis.

Front. Endocrinol. 16:1620230. doi: 10.3389/fendo.2025.1620230.

COPYRIGHT

© 2025 Shi, Zou, Li, Liu, Hu, Li, Zhang, Chen, Wu, Wang and Jin. This is an open-access article distributed under the terms of the Creative Commons Attribution License (CC BY). The use, distribution or reproduction in other forums is permitted, provided the original author(s) and the copyright owner(s) are credited and that the original publication in this journal is cited, in accordance with accepted academic practice. No use, distribution or reproduction is permitted which does not comply with these terms.

SGLT2 inhibition attenuates diabetic tubulopathy by suppressing SGK1-mediated pyroptosis

Xu Shi^{1,2†}, Wei Zou^{3†}, Xuehong Li^{1,2}, Sirui Liu^{1,2}, Tiantian Hu^{1,2}, Qiong Li^{1,2}, Ting Zhang^{1,2}, Lei Chen^{1,2}, Sumin Wu^{1,2}, Cheng Wang^{1,2*} and Yongjie Jin^{1,2*}

¹Division of Nephrology, Department of Medicine, The Fifth Affiliated Hospital Sun Yat-Sen University, Zhuhai, China, ²Guangdong Provincial Key Laboratory of Biomedical Imaging, The Fifth Affiliated Hospital Sun Yat-Sen University, Zhuhai, China, ³Department of Nephrology, The University of Tokyo Hospital, The University of Tokyo, Tokyo, Japan

Background: Diabetic tubulopathy is increasingly recognized as a pivotal contributor to diabetic kidney disease (DKD) progression. Excessive pyroptosis of renal tubular epithelial cells exacerbates inflammation and tissue injury. Although sodium-glucose cotransporter 2 (SGLT2) inhibitors confer renal protection, their mechanistic linkage to pyroptosis remains unclear.

Methods: Renal biopsies from DKD patients, STZ-induced diabetic mice, and high glucose (HG)-stimulated HK-2 cells were analyzed. Pyroptosis markers and SGK1 signaling were assessed following SGLT2 knockdown, overexpression, or treatment with SGLT2 inhibitor empagliflozin (EMPA) and the SGK1 inhibitor EMD638683 (EMD).

Results: SGLT2 and Gasdermin D N-terminal domain (GSDMD-N) were upregulated in DKD kidneys and correlated with tubular injury and renal dysfunction. EMPA reduced pyroptosis marker expression, tubular injury, and fibrosis in diabetic mice. *In vitro*, HG induced SGLT2 upregulation, SGK1 activation, and pyroptosis in HK-2 cells, which were reversed by EMPA. SGLT2 overexpression increased SGK1 and pyroptosis even under normoglycemia, while SGK1 inhibition suppressed HG-induced pyroptosis and NF-κB activation. **Conclusion:** SGLT2 promotes diabetic tubular injury through SGK1-mediated pyroptosis. Inhibition of the SGLT2/SGK1 axis alleviates pyroptosis and offers a potential therapeutic strategy for DKD.

KEYWORDS

diabetic tubulopathy, SGLT2, SGK1, pyroptosis, inflammation

1 Introduction

Diabetic kidney disease (DKD), one of the most prevalent microvascular complications of diabetes worldwide, is a leading cause of end-stage renal disease (ESRD) (1). Traditionally, glomerular injury has been regarded as the primary site of damage in DKD, with progressive glomerular dysfunction driving proteinuria and a gradual decline in renal function (2–4). However, advancing research on DKD challenges this paradigm, suggesting that glomerular injury may not be the decisive factor in disease initiation or progression, nor the earliest event in diabetic renal injury (5, 6). Recent studies increasingly highlight the critical role of tubular pathology, particularly proximal tubular injury, in DKD progression—a phenomenon termed "diabetic tubulopathy" (7, 8).

Emerging therapeutic strategies for DKD increasingly focus on targeting tubular injury. Sodium-glucose cotransporter 2 (SGLT2) inhibitors, a unique class of antidiabetic agents primarily targeting renal tubules (9), ameliorate renal injury through glycemic control, hemodynamic modulation, metabolic regulation, sodium load reduction, and anti-inflammatory actions (10-13). Intriguingly, the anti-inflammatory benefits of SGLT2 inhibitors appear independent of their glucose-lowering effects. Randomized, double-blind, placebocontrolled, multicenter clinical trials, such as EMPA-KIDNEY, DAPA-CKD, and EMPA-HF have demonstrated that SGLT2 inhibitors exert cardiovascular and renal protective effects in both diabetic and non-diabetic populations, significantly improving patient outcomes (14-16). Transcriptomic analyses suggest that the glucose-independent renoprotection of SGLT2 inhibitors is associated with serum- and glucocorticoid-regulated kinase 1 (SGK1) (17), though further mechanistic validation is needed.

Excessive and persistent pyroptosis triggers severe inflammatory responses (18, 19). The canonical pyroptosis pathway mediated by the NOD-like receptor family pyrin domain-containing 3 (NLRP3) inflammasome plays a critical regulatory role in diseases such as DKD, obstructive nephropathy, lupus nephritis, and renal fibrosis (20, 21). Genetic ablation of NLRP3 has been demonstrated to ameliorate renal inflammation and fibrosis in diabetic mice models (22). While inflammasomes are classically associated with immune cells (e.g., mast cells, lymphocytes, and macrophages), renal tubular epithelial cells (RTECs) also express functional inflammasomes capable of secreting pro-inflammatory cytokines, positioning pyroptosis inhibition as a therapeutic strategy for diabetic tubulopathy (11, 23). RTECs act as both victims and active contributors to inflammation. Elucidating SGLT2-mediated injury mechanisms in RTECs may advance therapeutic strategies for diabetic tubulopathy.

2 Materials and methods

2.1 Human kidney biopsies and urine samples

All human samples (renal biopsies or urine) were collected from patients at the Fifth Affiliated Hospital Sun Yat-sen University after

obtaining written informed consent. This study enrolled male or female patients aged ≥18 years with type 2 diabetes mellitus (T2DM), defined by the American Diabetes Association's 2010 Standards of Medical Care in Diabetes, and biopsy-confirmed diabetic kidney disease (DKD) meeting the new pathological classification criteria provided by the Renal Pathology Society. Patients with severe non-diabetic kidney diseases, renal artery stenosis, uncontrolled hypertension, chronic heart failure with persistent symptoms, or those using SGLT2 inhibitors were excluded. Five kidney samples from tumor nephrectomy patients without diabetes or kidney diseases served as normal controls. Twenty renal biopsy samples from T2DM patients with biopsyproven DKD were clinically characterized by persistent albuminuria (>300 mg/24 h). Demographic and clinical data of DKD patients are summarized in Supplementary Table S1. For urine samples, 50 mL of clean morning urine was collected from 28 biopsy-confirmed DKD patients with T2DM and 18 healthy subjects during routine physical examinations. Demographic and clinical data of DKD patients and healthy controls are presented in Supplementary Table S2. This study was approved by the Ethics Committee of the Fifth Affiliated Hospital Sun Yat-sen University (Approval No.: 2022#K180-1).

2.2 Animal models

The research involving murine models was approved by the Institutional Animal Care and Use Committee of the Fifth Affiliated Hospital Sun Yat-sen University (Approval No. 00314, Guangdong, China). Four-week-old healthy male C57BL/6J mice were purchased from the Guangdong Medical Laboratory Animal Center (Foshan, Guangdong). All mice were fed either a high-fat diet (HFD; 60 kcal% from fat, D12492, Research Diets) or a standard chow diet (12 kcal% from fat) and housed under con-trolled temperature conditions (22-26 °C) with a 12-hour light/dark cycle. After six weeks of HFD feeding, diabetes was induced in the mice by intraperitoneal injection of streptozotocin (STZ) (S0130, Sigma-Aldrich) (20). Before receiving daily STZ injections, the mice were fasted for 12 hours. STZ was administered intraperitoneally at a dose of 50 mg/kg body weight for five consecutive days. Control mice received an equal volume of 0.1 mol/L citrate buffer (pH = 4.5) simultaneously. One week after the last injection, blood samples were collected from the tail vein of all mice to measure fasting blood glucose levels. Mice with fasting blood glucose levels ≥ 300 mg/dL were considered diabetic (marked as week 0).

Mice were divided into four groups: control group, empagliflozin (EMPA) group, STZ-induced diabetes group, and STZ-induced diabetes + EMPA treatment group, with 6 mice in each group. Starting from the day fasting blood glucose testing con-firmed the successful establishment of the diabetes model (designated as week 0) until euthanasia (designated as week 12), mice were administered EMPA (HY-15409, MedChemExpress) via oral gavage at a dose of 10 mg/kg/day. Control group mice received an equal volume of 0.9% normal saline via oral gavage daily for 12 weeks.

2.3 Renal function

Serum creatinine levels were determined using a Creatinine Assay Kit (sarcosine oxidase) (C011-2-1, Nanjing Jiancheng Bioengineering Institute) following the manufacturer's instructions. Similarly, Blood urea nitrogen concentrations were measured with a Urea Nitrogen Colorimetric Detection Kit (C013-2-1, Nanjing Jiancheng Bioengineering Institute) in accordance with the provided protocol.

2.4 Cell culture and treatment

The HK-2 cells (CRL-2190, ATCC) were cultured in DMEM/ F12 medium (C11330500BT, GIBCO) supplemented with 10% FBS (C04001, Vivacell), 100 U/mL penicillin, and 100 mg/mL streptomycin (C3420-0100, Vivacell) and maintained at 37°C in a humidified incubator with 5% CO2. HK-2 cells were treated for 24-72 hours with either normal glucose (NG) medium (5.5 mmol/L D-glucose + 24.5 mmol/L mannitol) or high glucose (HG) medium (30 mmol/L D-glucose). SGLT2 siRNA and negative control siRNA were purchased from HanYi Bio (Guangzhou, China). The siRNA sequences used were as follows: SGLT2 sense, AGAAGGCCCUGAUU-GACAATT; SGLT2 antisense, UUGUCAAUCAGGGCCUUCUTT. The SGLT2 (SLC5A2)-3×Flag plasmid was also obtained from HanYi Bio and constructed using the pcDNA3.1 vector, with the pcDNA3.1-3×Flag plasmid serving as a negative control. siRNA and plasmid transfections were performed using Lipofectamine TM 3000 (L3000015, Thermo Fisher Scientific) according to the manufacturer's instructions. To examine the inhibitory effects of empagliflozin (HY-15409, MedChemExpress) and EMD638683 (EMD) (HY-15193, MedChemExpress) on pyroptosis, HK-2 cells were treated with HG in the presence of EMPA (500 nM) or EMD (50 µM). After 72 hours of incubation, cells were collected for further analysis.

2.5 Measurement of interleukin- 1β , interleukin-18, and lactate dehydrogenase

The IL-1 β and IL-18 enzymatic activity in urine and cell culture medium were assayed using a IL-1 β Elisa Kit (EK0392,` BOSTER Company) and IL-18 (EK0864, BOSTER Company) following the manufacturer's instructions. The LDH release in cell culture medium was conducted by the manufacturer's instructions.

2.6 Cell viability assay

The CCK-8 assay was used to assess cell viability by measuring dehydrogenase activity in live cells. HK-2 cells were seeded into 96-well plates and cultured until reached 80–90% confluency. The cells were treated with indicated agents under NG or HG conditions. To evaluate cell viability, 10 μ L CCK-8 solution (CK04, Dojindo) was

added to each well, followed by incubation for 2 h at 37 °C. Absorbance was measured at 450 nm wavelength using a microplate reader (EnVision).

2.7 Periodic acid—Schiff staining and quantitative assessment of tubular injury

PAS staining was used to assess tubular morphological changes and degree of injury. PAS staining was performed following the manufacturer's instructions (DG0005, Leagene Biotech). Paraffinembedded tissue sections were deparaffinized and rehydrated through sequential immersion in xylenes, graded ethanol solutions, and water, as previously described (24, 25). Oxidation was performed using 0.5% periodic acid solution for 8 minutes, followed by rinsing under running tap water for 5 minutes. Sections were then incubated with Schiff reagent for 15 minutes until a light pink coloration developed. After counterstaining with hematoxylin, the sections were dehydrated, cleared, and mounted with coverslips. Tubular injury was assessed based on morphological changes including tubular dilation or atrophy, cast formation, vacuolization, epithelial cell shedding, brush border loss, and basement membrane thickening. Tubular injury was evaluated using a semi-quantitative scoring system: 0 = no injury; $1 = \le 10\%$ injured tubules; 2 = 11%-25%; 3 = 26%-50%; 4 = 51%-74%; and 5 =≥75% injured (26).

2.8 Masson's trichrome staining

Masson's trichrome staining was applied to evaluate interstitial fibrosis, a hallmark of progressive kidney damage. The staining procedure was performed according to the manufacturer's guidelines (DC0033, Leagene Biotech). Briefly, paraffin-embedded tissue sections underwent sequential deparaffinization through a graded series of xylenes and ethanol solutions followed by hydration in distilled water. Sections were incubated in Weigert's iron hematoxylin for 5 minutes at room temperature, then thoroughly washed under running tap water. Subsequently, samples were immersed in Biebrich scarlet-acid fuchsin staining solution for 10 minutes. Differentiation was achieved by treating slides with a phosphomolybdic-phosphotungstic acid mixture for 10 minutes, followed by counter-staining with aniline blue solution. A brief 10-second acid alcohol rinse was applied to optimize cytoplasmic staining. Finally, tissues were dehydrated through an ascending ethanol series, cleared in xylene, and permanently mounted with a synthetic resin-based medium.

2.9 Immunohistochemistry staining

Kidney injury molecule-1 (KIM-1) is a well-recognized biomarker of tubular damage. We assessed renal injury severity through KIM-1 immunostaining. The paraffin sections were deparaffinized and rehydrated as previously described.

Deparaffinized tissue sections ($4\mu m$) were prepared, and antigen retrieval was performed using citrate buffer (10~mM, C1032, Solarbio Life Sciences) in an autoclave at $120~^{\circ}C$ for 10~min. Endogenous peroxidase activity was blocked with $1\%~H_2O_2$ for 10~min. After blocking with 10%~donkey serum, sections were incubated overnight at $4~^{\circ}C$ with anti-Kim-1(R&D systems, AF1817, RRID: AB_2116446, 1:200), followed by a 1~h incubation with biotinylated secondary antibodies at room temperature and an additional 1~h incubation with HRP Conjugated Streptavidin Complex (BA1088, Boster). DAB was used for visualization, and hematoxylin was applied as a counterstain. Images were acquired using All-in-One Fluorescence Microscope (BZ-X Itasca).

2.10 Immunofluorescence staining

After antigen retrieval, sections were blocked with 5% donkey serum and incubated with primary antibodies overnight at 4°C: anti-SGLT2 (Abcam, sc-393350, RRID: AB_2814658, 1:200), anti-GSDMD-N (Proteintech, 66387-1-IG, RRID: AB_2881763, 1:200), anti-p-SGK1 (Affinity Biosciences, AF3001, RRID: AB_2834440, 1:200), and anti-F4/80 (CST, 70076T, RRID: AB_2799771, 1:200). Alexa Fluor 488(abcam, ab150160, RRID: AB_2756445)/594 (abcam, ab150077, RRID: AB_2630356) secondary antibodies were used and nuclei were counterstained with DAPI (HYD0814, MCE). Images were acquired on a Pannoramic 250 FLASH III scanner (3DHISTECH).

2.11 Immunoblotting

Immunoblotting was performed as previously described (22, 23). Briefly, the tis-sues/cells were homogenized and lysed in a lysis buffer containing protease and phosphatase inhibitors. The same amounts of protein were electrophoresed by sodium dodecyl sulfate-polyacrylamide (SDS-PAGE) gel and then transferred to PVDF mem-branes (Millipore-Sigma). The membrane blotting was performed using 5% nonfat milk for 1 h at room temperature, and then the membranes were incubated with the primary antibodies overnight at 4 °C. After washing with TBST, the membranes were incubated with HRP-conjugated goat anti-rabbit or goat anti-mouse secondary antibodies for 1 h. The signals were captured using a SuperSignal West Femto Maximum Sensitivity Substrate kit (Thermo Scientific).

The following antibodies were used in this study: anti-SGLT2 (SANTA CRUZ, sc-393350; RRID: AB_2814658, 1:1000), Cleaved Caspase-1 (CST, 4199S; RRID: AB_1903916, 1:2000), GSDMD-N (Proteintech, 66387-1-IG; RRID: AB_2881763, 1:2000), IL-1β(Abcam, ab9722; RRID: AB_308765, 1:2000), IL-18 (Abcam, ab191152, RRID: AB_2737346. 1:2000), α-tubulin(Ribobio, CRM2007, AB_2934267, 1:5000), phospho-SGK1 (Ser422) (Affinity Biosciences, AF3001, RRID: AB_2834440, 1:1000), SGK1 (CST, 12103S, RRID: AB_2687476, 1:2000), β-actin(HUABIO, HA722023, AB_3096833, 1:10,000), phospho-NF-κb(S536) (CST, 3033T, RRID: AB_331284, 1:2000), Nlrp3(CST, 15101S, RRID:

AB_2722591, 1:2000), goat anti-rabbit secondary antibody (Abcam, ab205718, AB_2819160); and goat anti-mouse secondary antibody (Abcam, ab205719, RRID:AB_2755049).

2.12 Quantitative real-time polymerase chain reaction

Total RNA was extracted from HK-2 cells and mouse renal tissue using TRIzol reagent (15596026, Thermo Fisher Scientific). RNA purity and concentration were assessed using a NanoDrop 2000 spectrophotometer (Thermo Fisher Scientific). cDNA synthesis was carried out with the PrimeScript RT Reagent Kit (RR047A, TaKaRa Bio-technology) following the manufacturer's protocol. Quantitative real-time PCR was performed on a CFX96 Touch Real-Time PCR Detection System (Bio-Rad) using a reaction mixture containing 12.5 µL of TB Green Premix Ex Taq II (Tli RNaseH Plus) (RR820A, TaKaRa Biotechnology), 0.4 µM of SGLT2 primers (Forward: 5'-TCCTGCTGACATCCTAGTCATT-3', Reverse: 5'-GAAGAGCGCATTCCACTCG-3'), 2 µL of cDNA, and 8.5 µL of nuclease-free water. The thermal cycling program included an initial denaturation at 95 °C for 30 s, followed by 40 cycles of 95 °C for 5 s and 60 °C for 30 s. Gene expression levels were normalized to β-actin as an internal refer-ence and analyzed using the $2^-\Delta\Delta Cq$ method in Microsoft Excel.

2.13 Terminal deoxynucleotidyl transferase dUTP nick end labeling

Since random DNA fragmentation occurs during pyroptosis, TUNEL staining can be used to detect it (27, 28). A TUNEL BrightGreen Apoptosis Detection Kit (A112, Vazyme) was used ac-cording to the manufacturer's instructions. Briefly, HK-2 cells were cultured on TC-treated coverslips and subjected to highglucose (HG) treatment. After treatment, the coverslips were rinsed twice with PBS and fixed in 4% paraformaldehyde for 25 minutes at room temperature. The fixed cells were then permeabilized with 0.2% Tri-ton X-100 for 5 minutes, followed by equilibration in equilibration buffer for 30 minutes. Subsequently, the cells were incubated with 50 µL of the TdT reaction mixture at 37 °C for 60 minutes in the dark. After counterstaining with DAPI, images were acquired using All-in-One Fluorescence Microscope (BZ-X Itasca). For quantification, nine randomly selected non-overlapping fields of view were analyzed per sample. The number of TUNEL-positive cells and total cells were counted using ImageJ software, and the percentage of TUNEL-positive cells was calculated for statistical analysis.

2.14 Flow cytometric analysis of pyroptotic cells

Pyroptotic cells show a rapid Annexin V^+/PI^+ shift, due to the increased permeability of cell membranes, which allows the

detection of pyroptotic cells using flow cytometry (27). HK-2 cells (2×10^5 cells/well) were harvested using 0.25% trypsin without EDTA for 2 minutes. Apoptosis was assessed using the Annexin V-FITC/PI Apoptosis Detection Kit (A211, Vazyme, Nanjing, China) according to the manufacturer's instructions. Cells were double-stained with Annexin V-FITC and propidium iodide (PI) and subsequently analyzed by flow cytometry (CytoFlex LX, Beckman, USA). For each sample, 10^5 cells were analyzed, and each experimental condition was performed in triplicate. The percentage of pyroptotic cells was determined using FlowJo v10 software, with double-positive (Annexin V-FITC+/PI+) cells considered as pyroptotic.

2.15 Statistical analyses

Quantitative results are expressed as mean values \pm standard error of the mean (SEM). Intergroup differences were assessed as follows: Two-group comparisons: Student's t-test (unpaired, two-tailed) was employed. Multi-group comparisons: One-way or two-way analysis of variance (ANOVA) was selected based on experimental design, followed by Tukey's *post hoc* test for pairwise significance evaluation when ANOVA indicated global differences (p < 0.05). A significance threshold of p < 0.05 was applied across all analyses. Data processing and statistical computations were executed using GraphPad Prism V8 software (GraphPad Inc., San Diego, CA), with normality and homogeneity of variance verified prior to parametric testing.

3 Results

3.1 SGLT2 is associated with tubular epithelial cell pyroptosis and diabetic tubulopathy

To investigate the association between SGLT2 and pyroptosis, we performed dual immunofluorescence staining for SGLT2 and Gasdermin D N-terminal domain (GSDMD-N) in human renal biopsy specimens. The results demonstrated co-localization of SGLT2 and GSDMD-N in renal tubules of diabetic kidney disease (DKD) patients, with significantly increased expression compared to controls (Figures 1A-C). Since GSDMD-N-mediated pore formation facilitates the release of interleukin-1β (IL-1β) and IL-18—hallmark features of pyroptosis—we observed significantly elevated urinary IL-1β and IL-18 levels in DKD patients (Figures 1D, E). Additionally, clinical analysis revealed a positive correlation between SGLT2 expression and renal tubular injury markers, including plasma retinol-binding protein (RBP) and urinary N-acetyl-β-D-glucosaminidase (NAG) (Figures 1F, G). GSDMD-N expression also negatively correlated with estimated glomerular filtration rate (eGFR), and positively with serum creatinine (SCR), blood urea nitrogen (BUN), and urinary albumin-to-creatinine ratio (ACR) (Figures 1H-K), suggesting that SGLT2 may contribute to renal dysfunction in DKD through pyroptosis.

3.2 Empagliflozin attenuates tubular pyroptosis and ameliorates renal injury in STZ-induced diabetic mice

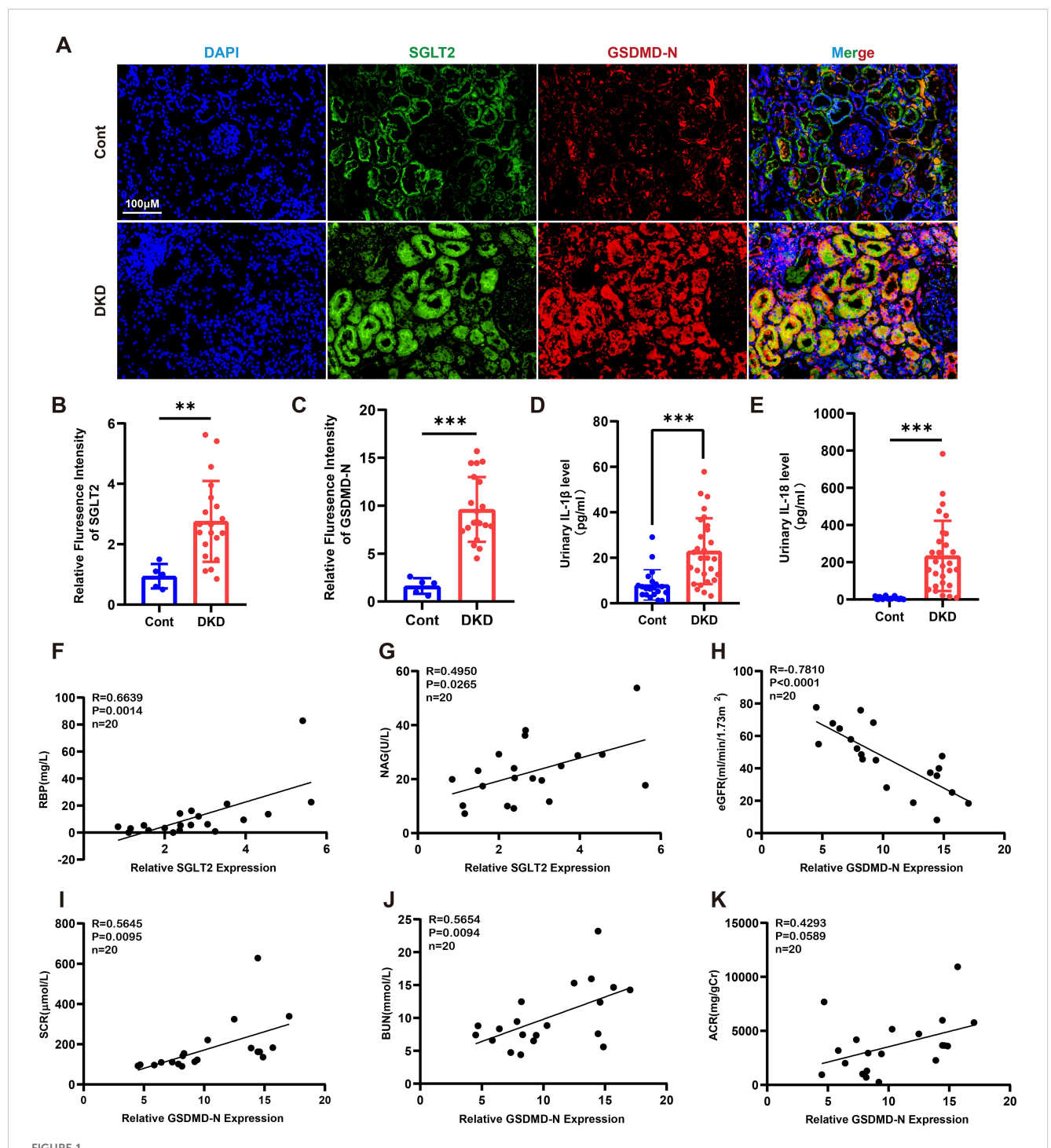
In streptozotocin (STZ)-induced diabetic mice, co-localization of SGLT2 and GSDMD-N was observed in renal tubules, with significantly increased expression compared to controls (Figures 2A–C). STZ mice showed elevated SCR, BUN, and urinary levels of IL-1 β and IL-18, all of which were mitigated by empagliflozin (EMPA) treatment (Figures 2D–G). Western blotting revealed marked upregulation of pyroptosis-related proteins (NLRP3, cleaved caspase-1, GSDMD-N, IL-1 β , and IL-18), which was reversed by EMPA (Figures 2H, I). Histological staining confirmed attenuation of tubular injury and interstitial fibrosis following EMPA therapy. Immunohistochemistry showed decreased expression of KIM-1 and reduced inflammatory cell infiltration in EMPA-treated mice (Figures 2J–N). These findings suggest that EMPA mitigates diabetic tubulopathy by suppressing tubular pyroptosis.

3.3 High glucose induces SGLT2 upregulation and pyroptosis in HK-2 cells

To further validate the association between SGLT2 and pyroptosis in renal tubular epithelial cells (RTECs), HK-2 cells were exposed to high glucose (HG, 30 mM) for 24–72 hours. Cell viability declined significantly after 48 hours and dropped to ~60% by 72 hours (Figure 3A). Lactate dehydrogenase (LDH), IL-1 β and IL-18 levels in the supernatant increased in a time-dependent manner (Figures 3B–D). Western blotting showed upregulation of SGLT2 and pyroptosis-related proteins, peaking at 72 hours (Figures 3E, F). DNA damage and membrane integrity disruption were confirmed via TUNEL and Annexin V-FITC/PI staining (27) (Figures 3G–J), establishing that HG induces pyroptosis in HK-2 cells, with 72-hour exposure as the optimal model condition.

3.4 Empagliflozin suppresses high glucoseinduced pyroptosis

To evaluate the anti-pyroptotic effects of SGLT2 inhibition, HK-2 cells under HG or NG conditions were treated with EMPA. EMPA significantly suppressed the HG-induced upregulation of NLRP3, cleaved caspase-1, GSDMD-N, IL-1β, and IL-18 (Figures 4A, E). It also reduced IL-1β, IL-18, and LDH release (Figures 4B-D). Moreover, EMPA treatment led to fewer TUNEL- and Annexin V-FITC/PI-positive cells under HG conditions (Figures 4F-I), confirming its *in vitro* anti-pyroptotic efficacy.

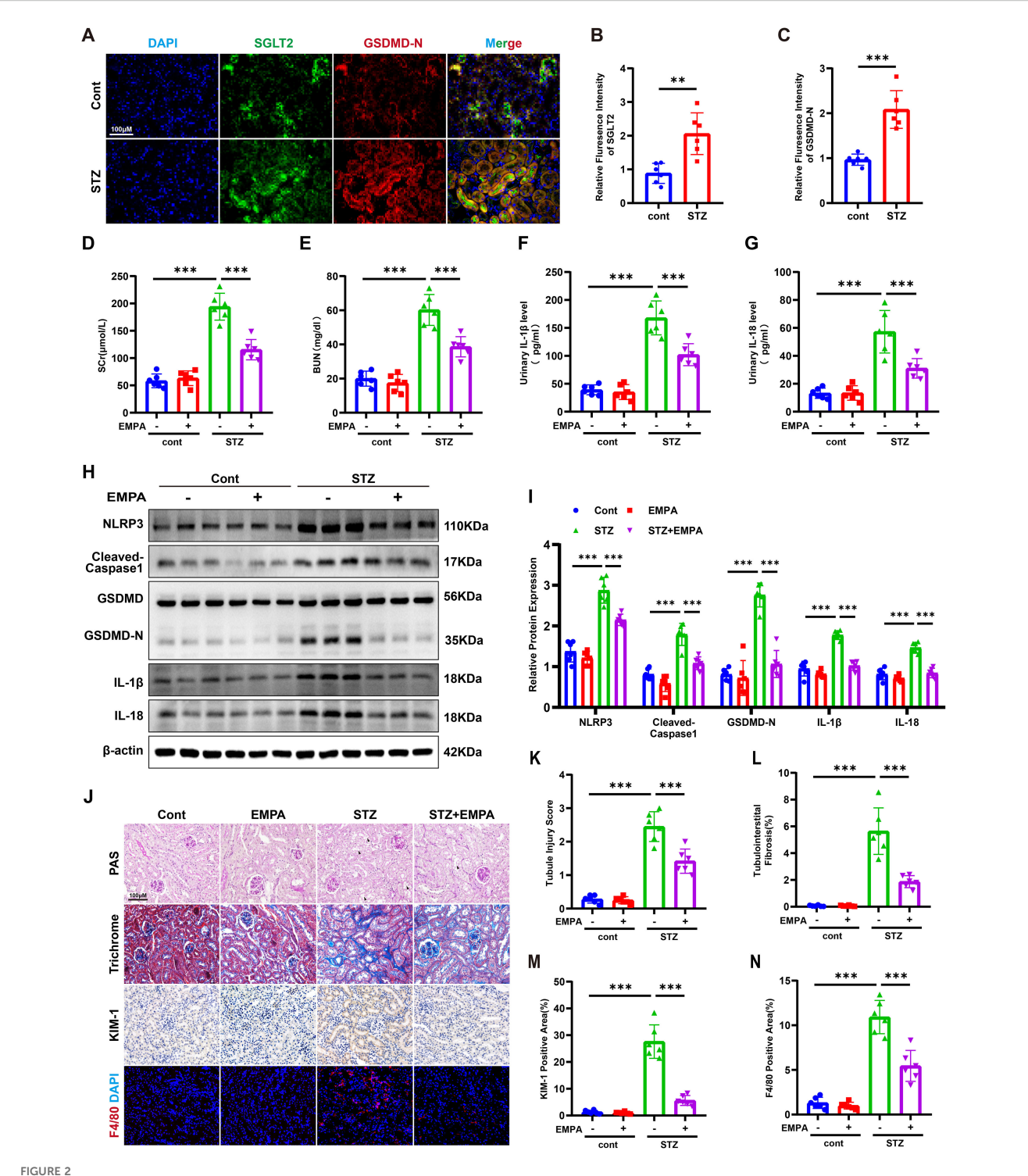


SGLT2 is associated with tubular epithelial cell pyroptosis and diabetic tubulopathy. (A) Representative immunofluorescence images showing co-localization of SGLT2 and GSDMD-N in kidney biopsies from DKD patients (n = 20) and paracancerous controls (n = 5). Original magnification, x400. (B, C) Quantification of SGLT2 (B) and GSDMD-N (C) expression in renal tubules. (D, E) Urinary IL-1 β (D) and IL-18 (E) levels in DKD patients (n = 28) and healthy controls (n = 20). (F, G) Correlation of SGLT2 expression with RBP (F) and NAG (G) in DKD patients (n = 20). (H-K) Correlation of GSDMD-N expression with eGFR (H), SCR (I), BUN (J), and ACR (K) in DKD patients (n = 20). Data are presented as mean \pm SEM. **p < 0.01, ***p < 0.001 by Student's t test (B-E) or Pearson correlation analysis (F-K).

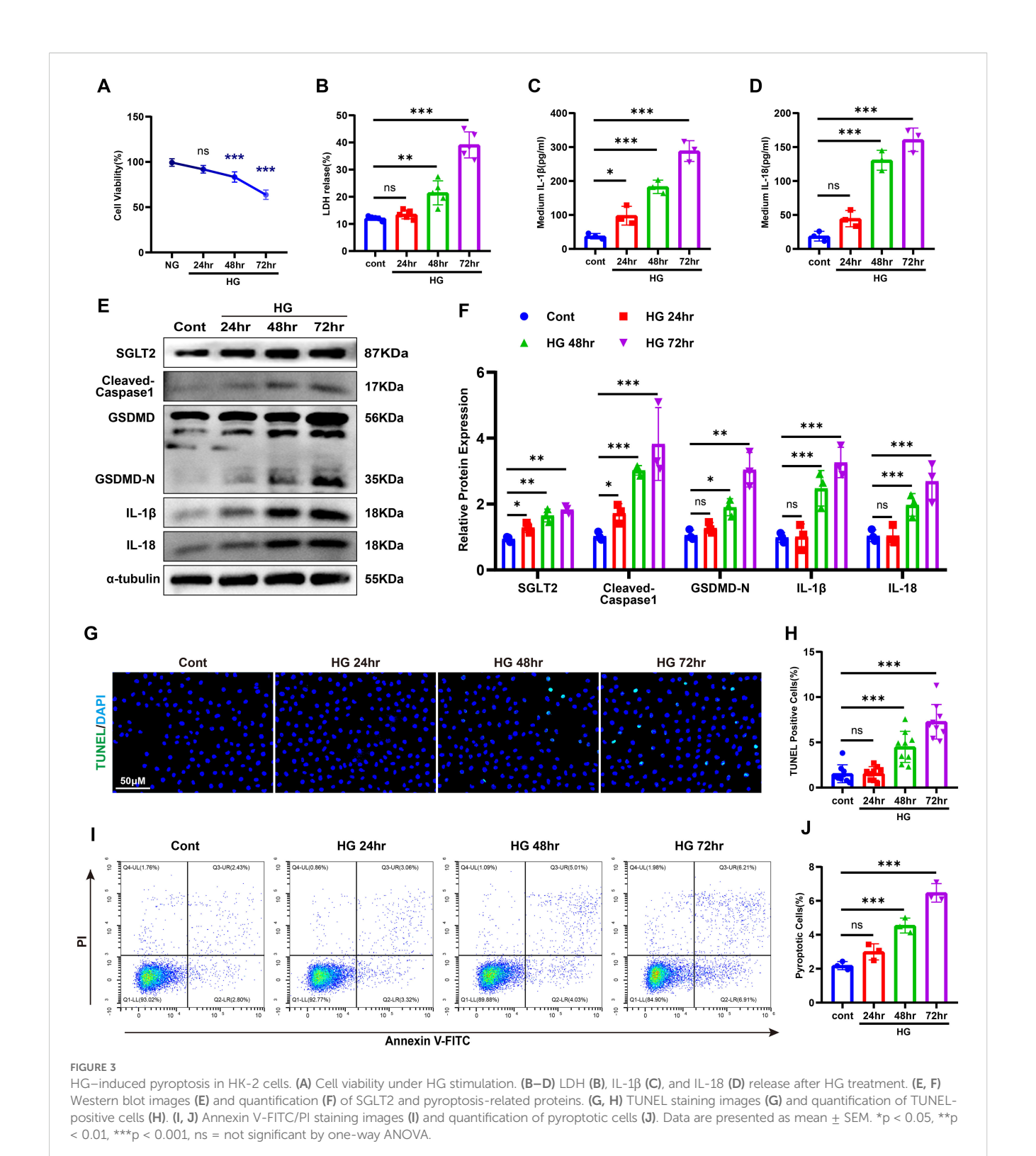
3.5 SGLT2 regulates SGK1 signaling and pyroptosis

To explore whether SGLT2 modulates pyroptosis, we performed knockdown and overexpression experiments (see Supplementary

Figure S1). SGLT2 knockdown attenuated HG-induced expression of cleaved caspase-1, GSDMD-N, IL-1 β , and IL-1 β , while overexpression increased these markers (Figures 5A–D). Given evidence implicating SGK1 in SGLT2i-mediated anti-inflammatory effects, we assessed SGK1 activation (17). In HG-treated HK-2 cells,



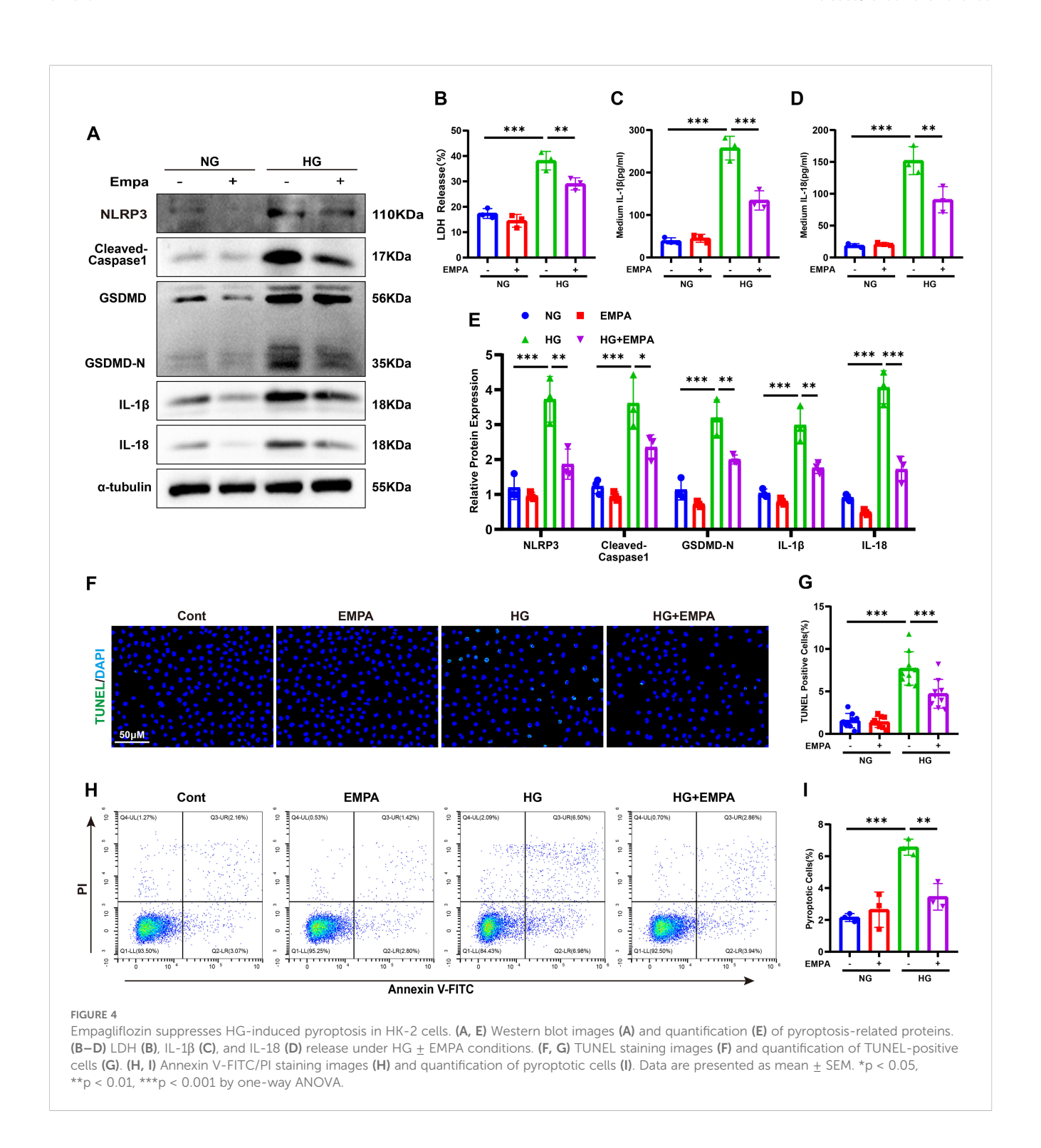
Empagiiflozin attenuates tubular pyroptosis and ameliorates renal injury in STZ-induced diabetic mice. (A) Representative immunofluorescence images of SGLT2 and GSDMD-N in kidneys of control and diabetic mice. Original magnification, x400. (B, C) Quantification of SGLT2 (B) and GSDMD-N (C) expression in renal tubules. (D, E) SCR (D) and BUN (E) levels. (F, G) Urinary IL-1 β (F) and IL-18 (G) levels. (H, I) Western blot images (H) and quantification (I) of pyroptosis-related proteins in kidney tissue. (J-N) Representative images of PAS staining (K), Masson's trichrome staining (L), immunohistochemistry for KIM-1 (M), and F4/80 immunofluorescence (N). Data are presented as mean \pm SEM. **p < 0.01, ***p < 0.001 by oneway ANOVA.



SGK1 and phosphorylated SGK1 (p-SGK1) increased in a time-dependent manner (Figures 5E–G), while EMPA treatment decreased both (see Supplementary Figure S2). Co-localization of SGLT2 and p-SGK1 was also observed in renal tubules of STZ-induced mice (Figures 5H–J). Notably, SGLT2 overexpression upregulated SGK1 phosphorylation even in normoglycemic conditions, suggesting SGLT2 directly regulates SGK1 signaling to promote pyroptosis.

3.6 SGK1 inhibition attenuates pyroptosis

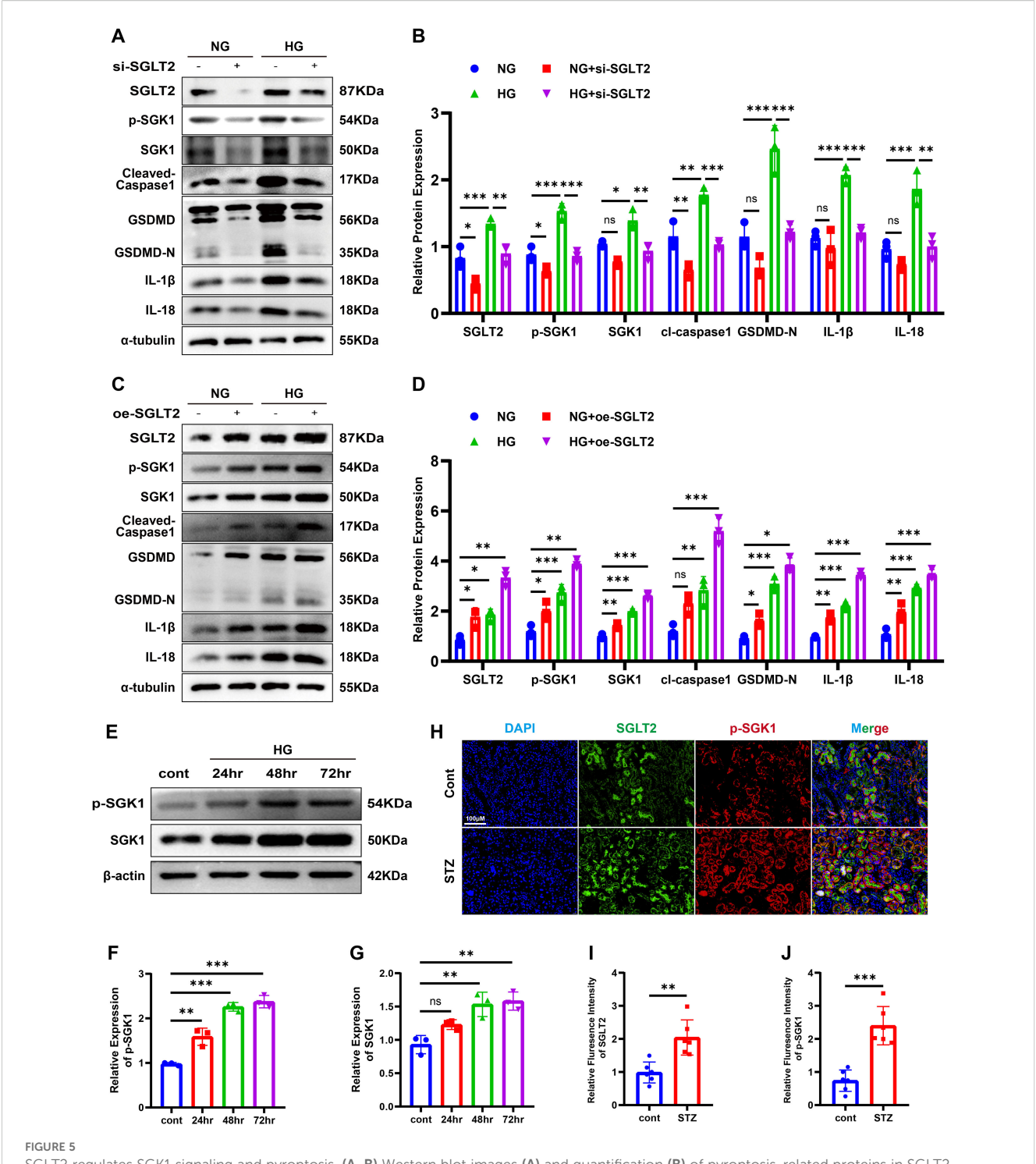
SGK1 is known to regulate nuclear factor kappa-light-chainenhancer of activated B cells (NF- κ B), particularly its p65 (RelA) subunit, which drives NLRP3 inflammasome expression (29). To assess the role of SGK1 in tubular pyroptosis, we treated HG-stimulated HK-2 cells with EMD638683 (EMD), a selective SGK1



inhibitor. EMD reversed HG-induced upregulation of p-p65, NLRP3, cleaved caspase-1, GSDMD-N, IL-1 β , and IL-18 (Figures 6A, E). LDH release and secretion of IL-1 β /IL-18 were also reduced (Figures 6B-D). Additionally, EMD significantly decreased the proportion of TUNEL- and Annexin V-FITC/PI-positive cells (Figures 6F-I). These results demonstrate that SGK1 is a critical mediator of SGLT2-induced pyroptosis.

4 Discussion

Here, we demonstrate that SGLT2 promotes pyroptosis in RTECs through activation of the SGK1 pathway, contributing to diabetic tubulopathy. In DKD patients and STZ-induced mice, SGLT2 co-localized with GSDMD-N in renal tubules, accompanied by elevated urinary IL-1 β and IL-18 and impaired

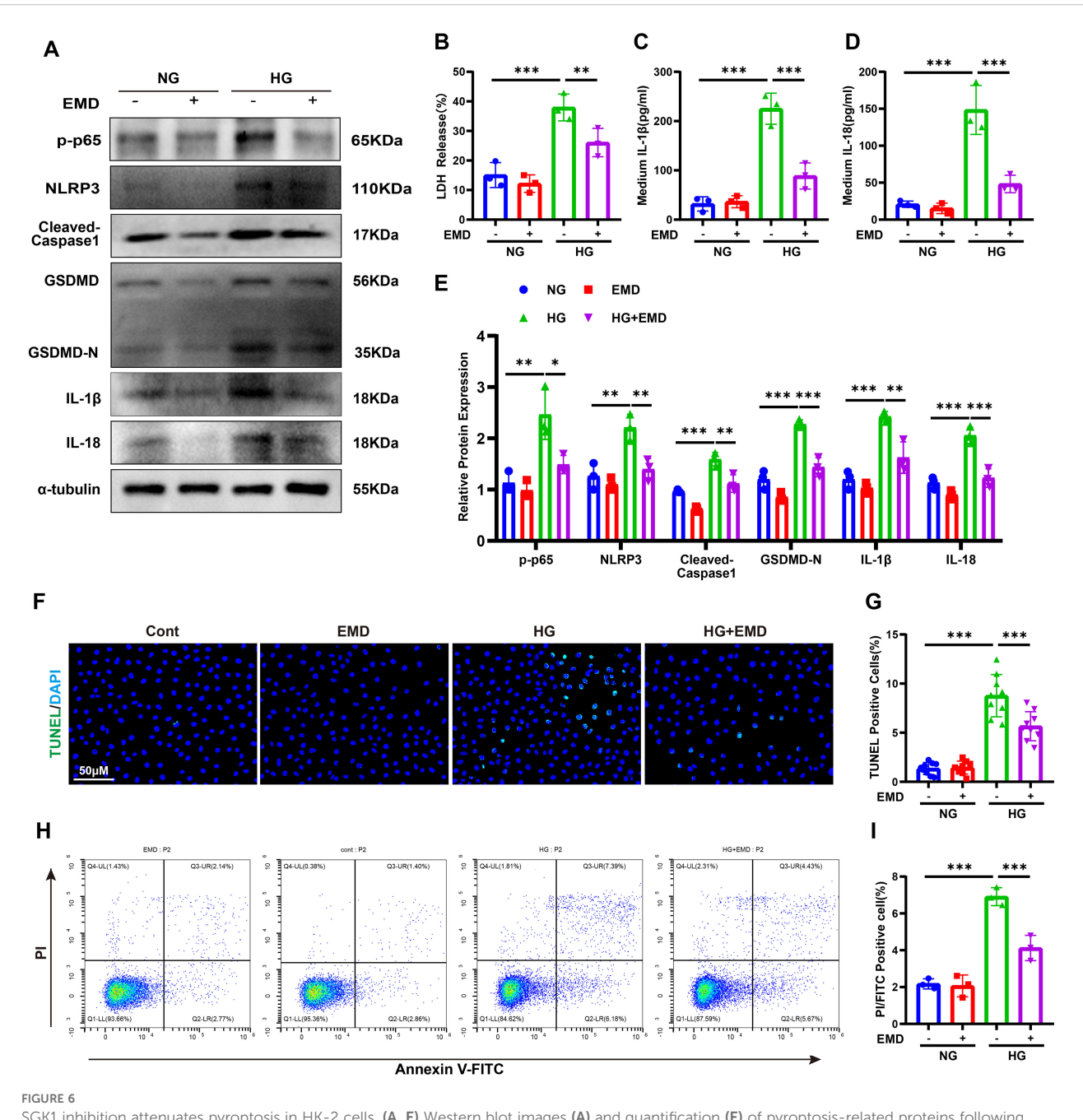


SGLT2 regulates SGK1 signaling and pyroptosis. (A, B) Western blot images (A) and quantification (B) of pyroptosis-related proteins in SGLT2 knockdown cells. (C, D) Western blot images (C) and quantification (D) in SGLT2-overexpressing cells. (E-G) Western blot images (E) and quantification of p-SGK1 (F) and total SGK1 (G) in a time-dependent manner following HG stimulation. (H-J) Representative immunofluorescence images showing co-localization of SGLT2 and p-SGK1 in kidneys (H) and their quantification (I, J). Original magnification, \times 400. Data are presented as mean \pm SEM. *p < 0.05, **p < 0.01, ***p < 0.001, ns = not significant by one-way ANOVA or t test.

renal function. HG induced SGLT2 and pyroptosis-related proteins in HK-2 cells, while EMPA or SGLT2 knockdown suppressed these effects. EMPA also reduced tubular injury and inflammation in diabetic mice. Mechanistically, SGLT2 enhanced SGK1 phosphorylation and pyroptosis, even under normoglycemia,

whereas SGK1 inhibition by EMD reversed HG-induced pyroptosis. These findings reveal a novel SGLT2/SGK1-NLRP3 axis driving tubular injury and highlight its therapeutic relevance.

DKD has traditionally been attributed to glomerular injury, with progressive proteinuria and renal dysfunction considered



SGK1 inhibition attenuates pyroptosis in HK-2 cells. (A, E) Western blot images (A) and quantification (E) of pyroptosis-related proteins following SGK1 inhibition (EMD). (B–D) LDH (B), IL-1 β (C), and IL-18 (D) release under HG \pm EMD conditions. (F, G) TUNEL staining images (F) and quantification of TUNEL-positive cells (G). (H, I) Annexin V-FITC/PI staining images (H) and quantification of pyroptotic cells (I). Data are presented as mean \pm SEM. *p < 0.05, **p < 0.01, ***p < 0.001 by one-way ANOVA.

hallmarks of disease progression (2–4). However, this paradigm fails to explain clinical observations, including the absence of proteinuria in 20.5%–61% of diabetic patients prior to renal function decline, and the stronger correlation of renal insufficiency with tubular pathology (e.g., tubular atrophy and interstitial fibrosis) rather than glomerular changes (5, 6, 30). Under diabetic conditions, RTECs are exposed to high glucose concentrations from both the apical and basolateral sides but lack mechanisms to limit glucose uptake, resulting in intracellular glucose overload. This burden is mostly driven by upregulated

SGLT2, which enhances glucose and sodium reabsorption and promotes oxidative stress and inflammation. Based on these features, SGLT2 is thought to be closely linked to the development of diabetic tubulopathy (10, 31, 32).

Previous studies have demonstrated that empagliflozin attenuates cardiac dysfunction by reducing NLRP3 inflammasome activation in heart failure models, and that SGLT2 inhibitors counteract NLRP3 activation via the immunomodulatory metabolite itaconate in ischemia-reperfusion injury (IRI) models. While these findings support the anti-inflammatory effects of SGLT2 inhibitors in various

organs, research specifically linking SGLT2 activity to pyroptosis in diabetic renal tubular epithelial cells remains limited (33, 34). Notably, pyroptosis has emerged as a critical driver of DKD progression, largely due to its uniquely inflammatory nature. Unlike other forms of regulated cell death, pyroptosis leads to cell membrane rupture and the release of pro-inflammatory cytokines such as IL-1B and IL-18, thereby amplifying tubular inflammation and injury (18-21). Mechanistically, this process is initiated by the activation of NLRP3 inflammasomes in response to damage- or pathogen-associated molecular patterns (DAMPs or PAMPs), leading to caspase-1 activation. Caspase-1 subsequently cleaves GSDMD, producing the pore-forming N-terminal fragment (GSDMD-N) that facilitates cytokine release (18). Accumulating preclinical and clinical evidence reveals that SGLT2 inhibitors exert systemic and tissue-specific antiinflammatory effects by suppressing NLRP3 inflammasome activation (33-36). In this study, we observed co-localization of SGLT2 and GSDMD-N in renal tubules of both human DKD specimens and STZinduced diabetic mice, along with elevated urinary IL-1 β and IL-18. SGLT2 inhibition with empagliflozin reduced pyroptosis and improved renal function in diabetic mice. These findings support the hypothesis that pyroptosis, likely driven by SGLT2-mediated NLRP3 activation, contributes to diabetic tubulopathy and that SGLT2 inhibition may confer renoprotection by suppressing this process.

SGLT2 inhibitors have emerged as novel therapeutic agents for DKD. Findings from the clinical trials demonstrated that SGLT2 inhibitors improve both cardiovascular and renal outcomes not only in diabetic patients but also in those without diabetes (14-16). These observations imply that the renoprotective effects of SGLT2 inhibition are not solely dependent on glucose control. It has been proposed that part of these benefits may be attributed to anti-inflammatory activity at the kidney level (37, 38); however, the underlying molecular mechanisms remain incompletely understood. Pirklbauer et al. (17) revealed through transcriptomic analyses that SGK1 may mediate glucose-independent anti-inflammatory mechanisms of SGLT2i. SGK1, a ubiquitously expressed serine/threonine kinase of the AGC family, is crucial for glucose homeostasis. Notably, SGK1 expression is characterized by remarkably high transcriptional volatility and is regulated by a variety of physiological and pathological stimuli, including hyperglycemia, cell shrinkage, ischemia, glucocorticoids, and mineralocorticoids (39, 40). SGK1 activation occurs downstream of insulin and various growth factors, primarily via the phosphatidylinositol 3-kinase (PI3K) pathway, involving 3phosphoinositide-dependent kinase-1 (PDK1) and mammalian target of rapamycin (mTOR). These features underscore SGK1 as a key metabolic and stress-responsive kinase, linking upstream signals such as hyperglycemia to downstream cellular processes including inflammation and cell death (39, 41). Mechanistically, SGK1 enhances NF-κB activity via phosphorylation of IKKα, and NF-κB—a master transcriptional regulator of inflammation-directly promotes the expression of NLRP3, GSDMD, IL-1β, and IL-18 (29, 42). In our study, we confirmed the co-localization of SGLT2 and SGK1 in the kidneys of STZ-induced diabetic mice. By knocking down or overexpressing SGLT2, we demonstrated that SGK1 is regulated by SGLT2. Consistently, overexpression of SGLT2 led to increased expression of SGK1 and pyroptosis markers even in the absence of high glucose stimulation. Our findings are in line with previous studies demonstrating the functional relevance of the SGLT2–SGK1 axis in diabetic kidney disease. For instance, SGLT2 knockdown has been shown to restore the Th17/Treg balance and attenuate diabetic nephropathy in *db/db* mice by regulating SGK1 via sodium signaling (43). These findings suggest that SGLT2 can directly induce pyroptosis in renal tubular epithelial cells via SGK1 activation, which may partially explain the renoprotective effects of SGLT2 inhibitors observed in non-diabetic patients. In addition, SGK1-mediated suppression of AMP-activated protein kinase activity may also be involved in the anti-inflammatory mechanisms of SGLT2 inhibitors, although this hypothesis requires further investigation (12, 13, 44).

Taken together, our study elucidates the critical role of SGLT2 in regulating pyroptosis in renal tubular epithelial cells and links it to the pathogenesis of diabetic tubulopathy. We demonstrate that SGLT2 inhibitors primarily suppress pyroptosis by modulating the SGK1 signaling pathway, and this protective effect appears to be independent of glucose levels. These findings not only deepen our understanding of the mechanisms underlying diabetic tubulopathy but also underscore the potential value of SGLT2 inhibitors as anti-inflammatory agents for treating renal tubular injury.

Data availability statement

The datasets presented in this study can be found in online repositories. The names of the repository/repositories and accession number(s) can be found below: DOI: 10.5281/zenodo.15163324.

Ethics statement

The studies involving humans were approved by Ethics Committee of the Fifth Affiliated Hospital Sun Yat-sen University (Approval No.: 2022#K180-1). The studies were conducted in accordance with the local legislation and institutional requirements. The participants provided their written informed consent to participate in this study. The animal study was approved by Institutional Animal Care and Use Committee of the Fifth Affiliated Hospital Sun Yat-sen University (Approval No. 00314, Guangdong, China). The study was conducted in accordance with the local legislation and institutional requirements.

Author contributions

YJ: Validation, Conceptualization, Project administration, Supervision, Writing – review & editing, Methodology, Writing – original draft, Data curation. XS: Validation, Data curation, Formal Analysis, Investigation, Writing – original draft. WZ: Formal Analysis, Writing – original draft, Validation, Investigation, Data curation. XL: Methodology, Writing – review & editing, Investigation. SL: Methodology, Writing – review & editing, Investigation. TH: Writing – review & editing, Methodology, Investigation. QL: Methodology, Investigation, Writing – review & editing. TZ:

Methodology, Investigation, Writing – review & editing. LC: Funding acquisition, Writing – review & editing. SW: Writing – review & editing, Funding acquisition. CW: Writing – review & editing, Resources, Supervision.

Funding

The author(s) declare financial support was received for the research and/or publication of this article. This work was funded by the Basic and Applied Basic and Applied Basic Research Foundation of Guangdong Province (Grants 2022A1515111116 and 2022A1515111069). We sincerely thank LC and SW for their generous support of this research.

Acknowledgments

We thank Shicong Song and Kangqiang Weng for their technical support.

Conflict of interest

The authors declare that the research was conducted in the absence of any commercial or financial relationships that could be construed as a potential conflict of interest.

References

- 1. Zheng Y, Ley SH, Hu FB. Global aetiology and epidemiology of type 2 diabetes mellitus and its complications. *Nat Rev Endocrinol.* (2018) 14:88–98. doi: 10.1038/nrendo.2017.151
- 2. Fang Y, Chen B, Liu Z, Gong AY, Gunning WT, Ge Y, et al. Age-related GSK3beta overexpression drives podocyte senescence and glomerular aging. *J Clin Invest.* (2022) 132:e141848. doi: 10.1172/JCJ141848
- 3. Liang X, Wang P, Chen B, Ge Y, Gong AY, Flickinger B, et al. Glycogen synthase kinase 3beta hyperactivity in urinary exfoliated cells predicts progression of diabetic kidney disease. *Kidney Int.* (2020) 97:175–92. doi: 10.1016/j.kint.2019.08.036
- 4. Thomas MC, Brownlee M, Susztak K, Sharma K, Jandeleit-Dahm KA, Zoungas S, et al. Diabetic kidney disease. *Nat Rev Dis Primers*. (2015) 1:15018. doi: 10.1038/nrdp.2015.18
- 5. Kramer HJ, Nguyen QD, Curhan G, Hsu CY. Renal insufficiency in the absence of albuminuria and retinopathy among adults with type 2 diabetes mellitus. *JAMA*. (2003) 289:3273–7. doi: 10.1001/jama.289.24.3273
- 6. Retnakaran R, Cull CA, Thorne KI, Adler AI, Holman RR, Group US. Risk factors for renal dysfunction in type 2 diabetes: U.K. Prospective Diabetes Study 74. *Diabetes*. (2006) 55:1832–9. doi: 10.2337/db05-1620
- 7. Yao L, Liang X, Qiao Y, Chen B, Wang P, Liu Z. Mitochondrial dysfunction in diabetic tubulopathy. *Metabolism*. (2022) 131:155195. doi: 10.1016/j.metabol.2022.155195
- 8. Goncalves-Dias C, Morello J, Correia MJ, Coelho NR, Antunes AMM, Macedo MP, et al. Mercapturate pathway in the tubulocentric perspective of diabetic kidney disease. *Nephron.* (2019) 143:17–23. doi: 10.1159/000494390
- 9. Wanner C, Inzucchi SE, Lachin JM, Fitchett D, von Eynatten M, Mattheus M, et al. Empagliflozin and progression of kidney disease in type 2 diabetes. *N Engl J Med.* (2016) 375:323–34. doi: 10.1056/NEJMoa1515920
- 10. Mashayekhi M, Safa BI, Gonzalez MSC, Kim SF, Echouffo-Tcheugui JB. Systemic and organ-specific anti-inflammatory effects of sodium-glucose cotransporter-2 inhibitors. *Trends Endocrinol Metab.* (2024) 35:425–38. doi: 10.1016/j.tem.2024.02.003

Generative AI statement

The author(s) declare that no Generative AI was used in the creation of this manuscript.

Any alternative text (alt text) provided alongside figures in this article has been generated by Frontiers with the support of artificial intelligence and reasonable efforts have been made to ensure accuracy, including review by the authors wherever possible. If you identify any issues, please contact us.

Publisher's note

All claims expressed in this article are solely those of the authors and do not necessarily represent those of their affiliated organizations, or those of the publisher, the editors and the reviewers. Any product that may be evaluated in this article, or claim that may be made by its manufacturer, is not guaranteed or endorsed by the publisher.

Supplementary material

The Supplementary Material for this article can be found online at: https://www.frontiersin.org/articles/10.3389/fendo.2025.1620230/full#supplementary-material

- 11. Faria J, Gerritsen KGF, Nguyen TQ, Mihaila SM, Masereeuw R. Diabetic proximal tubulopathy: Can we mimic the disease for *in vitro* screening of SGLT inhibitors? *Eur J Pharmacol.* (2021) 908:174378. doi: 10.1016/j.ejphar.2021.174378
- 12. Mazzieri A, Basta G, Calafiore R, Luca G. GLP-1 RAs and SGLT2i: two antidiabetic agents associated with immune and inflammation modulatory properties through the common AMPK pathway. *Front Immunol*. (2023) 14:1163288. doi: 10.3389/fimmu.2023.1163288
- 13. Marcon LM, Mazzieri A. Anti-inflammatory and anti-oxidative effects of GLP1-RAs and SGLT2i: the guiding star towards cardiovascular protection in type 2 diabetes. *Immuno*. (2025) 5:11. doi: 10.3390/immuno5010011
- 14. The E-KCG, Herrington WG, Staplin N, Wanner C, Green JB, Hauske SJ, et al. Empagliflozin in patients with chronic kidney disease. *N Engl J Med.* (2023) 388:117–27. doi: 10.1056/NEJMoa2204233
- 15. Heerspink HJL, Stefansson BV, Correa-Rotter R, Chertow GM, Greene T, Hou FF, et al. Dapagliflozin in patients with chronic kidney disease. N Engl J Med. (2020) 383:1436-46. doi: 10.1056/NEJMoa2024816
- 16. Packer M, Anker SD, Butler J, Filippatos G, Pocock SJ, Carson P, et al. Cardiovascular and renal outcomes with empagliflozin in heart failure. N Engl J Med. (2020) 383:1413–24. doi: 10.1056/NEJMoa2022190
- 17. Pirklbauer M, Sallaberger S, Staudinger P, Corazza U, Leierer J, Mayer G, et al. Empagliflozin inhibits IL-1beta-mediated inflammatory response in human proximal tubular cells. *Int J Mol Sci.* (2021) 22:5089. doi: 10.3390/ijms22105089
- 18. Zhu C, Xu S, Jiang R, Yu Y, Bian J, Zou Z. The gasdermin family: emerging therapeutic targets in diseases. *Signal Transduct Target Ther.* (2024) 9:87. doi: 10.1038/s41392-024-01801-8
- 19. Coll RC, Schroder K, Pelegrin P. NLRP3 and pyroptosis blockers for treating inflammatory diseases. *Trends Pharmacol Sci.* (2022) 43:653–68. doi: 10.1016/j.tips.2022.04.003
- 20. Fan Q, Li R, Wei H, Xue W, Li X, Xia Z, et al. Research progress of pyroptosis in diabetic kidney disease. *Int J Mol Sci.* (2024) 25:7130. doi: 10.3390/ijms25137130

21. Liu Y, Lei H, Zhang W, Xing Q, Liu R, Wu S, et al. Pyroptosis in renal inflammation and fibrosis: current knowledge and clinical significance. *Cell Death Dis.* (2023) 14:472. doi: 10.1038/s41419-023-06005-6

- 22. Wu M, Han W, Song S, Du Y, Liu C, Chen N, et al. NLRP3 deficiency ameliorates renal inflammation and fibrosis in diabetic mice. *Mol Cell Endocrinol.* (2018) 478:115–25. doi: 10.1016/j.mce.2018.08.002
- 23. Al Mamun A, Ara Mimi A, Wu Y, Zaeem M, Abdul Aziz M, Aktar Suchi S, et al. Pyroptosis in diabetic nephropathy. *Clin Chim Acta*. (2021) 523:131–43. doi: 10.1016/j.cca.2021.09.003
- 24. Li X, Li Q, Jiang X, Song S, Zou W, Yang Q, et al. Inhibition of SGLT2 protects podocytes in diabetic kidney disease by rebalancing mitochondria-associated endoplasmic reticulum membranes. *Cell Commun Signal*. (2024) 22:534. doi: 10.1186/s12964-024-01914-1
- 25. Song S, Hu T, Shi X, Jin Y, Liu S, Li X, et al. ER stress-perturbed intracellular protein O-glcNAcylation aggravates podocyte injury in diabetes nephropathy. *Int J Mol Sci.* (2023) 24:17603. doi: 10.3390/ijms242417603
- 26. Takaori K, Nakamura J, Yamamoto S, Nakata H, Sato Y, Takase M, et al. Severity and frequency of proximal tubule injury determines renal prognosis. *J Am Soc Nephrol.* (2016) 27:2393–406. doi: 10.1681/ASN.2015060647
- 27. Wang S, Liu Y, Zhang L, Sun Z. Methods for monitoring cancer cell pyroptosis. Cancer Biol Med. (2021) 19:398–414. doi: 10.20892/j.issn.2095-3941.2021.0504
- 28. Yu P, Zhang X, Liu N, Tang L, Peng C, Chen X. Pyroptosis: mechanisms and diseases. Signal Transduct Target Ther. (2021) 6:128. doi: 10.1038/s41392-021-00507-5
- 29. Tai DJ, Su CC, Ma YL, Lee EH. SGK1 phosphorylation of IkappaB Kinase alpha and p300 Up-regulates NF-kappaB activity and increases N-Methyl-D-aspartate receptor NR2A and NR2B expression. *J Biol Chem.* (2009) 284:4073–89. doi: 10.1074/jbc.M805055200
- 30. Dwyer JP, Parving HH, Hunsicker LG, Ravid M, Remuzzi G, Lewis JB. Renal dysfunction in the presence of normoalbuminuria in type 2 diabetes: results from the DEMAND study. *Cardiorenal Med.* (2012) 2:1–10. doi: 10.1159/000333249
- 31. DeFronzo RA, Reeves WB, Awad AS. Pathophysiology of diabetic kidney disease: impact of SGLT2 inhibitors. *Nat Rev Nephrol.* (2021) 17:319–34. doi: 10.1038/s41581-021-00393-8
- 32. Vallon V. The proximal tubule in the pathophysiology of the diabetic kidney. *Am J Physiol Regul Integr Comp Physiol.* (2011) 300:R1009–22. doi: 10.1152/ajpregu.00809.2010
- 33. Byrne NJ, Matsumura N, Maayah ZH, Ferdaoussi M, Takahara S, Darwesh AM, et al. Empagliflozin blunts worsening cardiac dysfunction associated with reduced NLRP3 (Nucleotide-binding domain-like receptor protein 3) inflammasome activation

- in heart failure. Circ Heart Fail. (2020) 13:e006277. doi: 10.1161/CIRCHEARTFAILURE.119.006277
- 34. Ke Q, Shi C, Lv Y, Wang L, Luo J, Jiang L, et al. SGLT2 inhibitor counteracts NLRP3 inflammasome via tubular metabolite itaconate in fibrosis kidney. *FASEB J.* (2022) 36:e22078. doi: 10.1096/fj.202100909RR
- 35. Birnbaum Y, Bajaj M, Yang HC, Ye Y. Combined SGLT2 and DPP4 inhibition reduces the activation of the nlrp3/ASC inflammasome and attenuates the development of diabetic nephropathy in mice with type 2 diabetes. *Cardiovasc Drugs Ther.* (2018) 32:135–45. doi: 10.1007/s10557-018-6778-x
- 36. Kim SR, Lee SG, Kim SH, Kim JH, Choi E, Cho W, et al. SGLT2 inhibition modulates NLRP3 inflammasome activity via ketones and insulin in diabetes with cardiovascular disease. *Nat Commun.* (2020) 11:2127. doi: 10.1038/s41467-020-15983-6
- 37. Ahluwalia TS, Ronkko TKE, Eickhoff MK, Curovic VR, Siwy J, Eder S, et al. Randomized trial of SGLT2 inhibitor identifies target proteins in diabetic kidney disease. *Kidney Int Rep.* (2024) 9:334–46. doi: 10.1016/j.ekir.2023.11.020
- 38. Bonnet F, Scheen AJ. Effects of SGLT2 inhibitors on systemic and tissue low-grade inflammation: The potential contribution to diabetes complications and cardiovascular disease. *Diabetes Metab.* (2018) 44:457–64. doi: 10.1016/j.diabet.2018.09.005
- 39. Noor S, Mohammad T, Ashraf GM, Farhat J, Bilgrami AL, Eapen MS, et al. Mechanistic insights into the role of serum-glucocorticoid kinase 1 in diabetic nephropathy: A systematic review. *Int J Biol Macromol.* (2021) 193:562–73. doi: 10.1016/j.ijbiomac.2021.10.165
- 40. Sierra-Ramos C, Velazquez-Garcia S, Vastola-Mascolo A, Hernandez G, Faresse N, Alvarez de la Rosa D. SGK1 activation exacerbates diet-induced obesity, metabolic syndrome and hypertension. *J Endocrinol.* (2020) 244:149–62. doi: 10.1530/JOE-19-0275
- 41. Lang F, Gorlach A, Vallon V. Targeting SGK1 in diabetes. Expert Opin Ther Targets. (2009) 13:1303–11. doi: 10.1517/14728220903260807
- 42. Gan W, Ren J, Li T, Lv S, Li C, Liu Z, et al. The SGK1 inhibitor EMD638683, prevents Angiotensin II-induced cardiac inflammation and fibrosis by blocking NLRP3 inflammasome activation. *Biochim Biophys Acta Mol Basis Dis.* (2018) 1864:1–10. doi: 10.1016/j.bbadis.2017.10.001
- 43. Wang D, Zhang Q, Dong W, Ren S, Wang X, Su C, et al. SGLT2 knockdown restores the Th17/Treg balance and suppresses diabetic nephropathy in db/db mice by regulating SGK1 via Na(). *Mol Cell Endocrinol.* (2024) 584:112156. doi: 10.1016/j.mce.2024.112156
- 44. Zhou B, Zhang Y, Li S, Wu L, Fejes-Toth G, Naray-Fejes-Toth A, et al. Serum-and glucocorticoid-induced kinase drives hepatic insulin resistance by directly inhibiting AMP-activated protein kinase. *Cell Rep.* (2021) 37:109785. doi: 10.1016/j.celrep.2021.109785